

---

This is an electronic reprint of the original article.  
This reprint may differ from the original in pagination and typographic detail.

Väisänen, Saija; Kosonen, Harri; Ristolainen, Matti; Vuorinen, Tapani

## Cellulose dissolution in aqueous NaOH–ZnO : effect of pulp pretreatment at macro and molecular levels

*Published in:*  
Cellulose

*DOI:*  
[10.1007/s10570-021-03779-w](https://doi.org/10.1007/s10570-021-03779-w)

Published: 01/05/2021

*Document Version*  
Publisher's PDF, also known as Version of record

*Published under the following license:*  
CC BY

*Please cite the original version:*  
Väisänen, S., Kosonen, H., Ristolainen, M., & Vuorinen, T. (2021). Cellulose dissolution in aqueous NaOH–ZnO : effect of pulp pretreatment at macro and molecular levels. *Cellulose*, 28(7), 4385-4396.  
<https://doi.org/10.1007/s10570-021-03779-w>



# Cellulose dissolution in aqueous NaOH–ZnO: effect of pulp pretreatment at macro and molecular levels

Saija Väisänen · Harri Kosonen · Matti Ristolainen · Tapani Vuorinen

Received: 15 October 2020 / Accepted: 16 February 2021 / Published online: 4 March 2021  
© The Author(s) 2021

**Abstract** This paper discusses the effect of hydrolytic pretreatments on pulp dissolution in the aqueous NaOH–ZnO solvent system. Eight samples were studied. They consisted of a never-dried softwood kraft pulp that was hydrolyzed under seven different conditions as well as the pulp without hydrolysis as a reference. The dissolution of the pulps was evaluated both at the macro level as well as at the molecular level based on their reactivity with 4-acetamido-2,2,6,6-tetramethylpiperidine-1-oxo-piperidinium (4-AcNH-TEMPO<sup>+</sup>). The fiber properties (i.e. the extent of fibrillation, amount of fines and fiber width, coarseness, and length) as well as the chemical composition (hemicellulose and cellulose contents) and the viscosity of the pulps was investigated. The results show that hydrolysis at medium consistency (10%) was successful in increasing the solubility of cellulose. Hydrolysis at high consistency (50%), on the other hand, increased the solubility only to some extent. With extended treatment time the fibers formed aggregates and their dissolution became poor. This phenomenon could be overcome by mechanically refining the fibers

after the hydrolysis. Moreover, comparison of the viscosity of the pulp over the degree of oxidation revealed that the viscosity needed to decrease below ca. 400 ml/g in order for the outer layers of the fibers to dissolve. Finally, when pulps with similar viscosities were compared against each other, the ones with the higher glucomannan contents formed gels over time. This was true also for the pulp with the lowest viscosity and the highest solubility of the studied samples.

**Keywords** Cellulose · Dissolution · Hydrolysis · Reactivity · TEMPO-oxidation

## Introduction

As renewable, recyclable, biocompatible and non-toxic substance, cellulose is a highly interesting raw material for manufacturing bio-based products. The utilization of the full potential of this natural polymer, however, often requires its dissolution, which is challenging. As the load-bearing structure in nature, cellulose is organized in the plant cell wall in a hierarchical arrangement that resists degradation. The stiffness of cellulose chains and their close packing make cellulose dissolution a difficult process. Moreover, cellulose is an amphiphilic molecule and therefore strong intra- and intermolecular hydrogen

S. Väisänen (✉) · T. Vuorinen  
Department of Bioproducts and Biosystems, School of  
Chemical Engineering, Aalto University, P.O. Box 16300,  
00076 Aalto, Finland  
e-mail: saija.vaisanen@aalto.fi

H. Kosonen · M. Ristolainen  
NE Research Center, UPM Pulp Research and  
Innovations, 53200 Lappeenranta, Finland

bonding as well as hydrophobic interactions between the molecules affect its solubility (Lindman et al. 2010; Medronho and Lindman 2015). Thus, cellulose is insoluble in water as well as in the most common organic solvents.

Dissolution of cellulose is, however, possible with certain solvents or solvent systems that are able to diffuse into the structure, disrupt the crystalline arrangement of the molecules as well as separate cellulose chains from each other (Ghasemi et al. 2017a, b). Cellulose dissolution with aqueous sodium hydroxide (NaOH) has a strong industrial potential due to the rapid, non-toxic, low cost and environmentally friendly process. The process has been known already since the early 1900s (Davidson 1934, 1936) and it continues attracting a lot of interest (Cai et al. 2008; Egal et al. 2007; Hagman et al. 2017; Huh et al. 2020; Kihlman et al. 2012; Medronho and Lindman 2015). The dissolution takes place at low temperature ( $< 0\text{ }^{\circ}\text{C}$ ) and hence there is no evaporation of chemicals during the process. The process is fast, however, moderately low degree of polymerization (DP), low cellulose concentration and narrow NaOH concentration range (7–10%) are required (Budtova and Navard 2016; Cai et al. 2008; Egal et al. 2007; Hagman et al. 2017; Isogai and Atalla 1998; Medronho and Lindman 2015). Moreover, semidilute solutions (e.g. 5% cellulose in 9% NaOH solution) tend to gel with time and increase in temperature (Liu et al. 2011; Pereira et al. 2018; Roy et al. 2003). Several mechanisms for cellulose dissolution in aqueous NaOH have been proposed. One of the theories suggests that at low temperatures NaOH forms hydrates with water that may permeate into the structure of the cellulosic material and detach individual cellulose chains from each other (Cai et al. 2008; Egal et al. 2007). On the other hand, it has been shown that cellulose deprotonates in aqueous NaOH (Bialik et al. 2016; Isogai 1997). Charging up polymers is expected to increase their solubility and thus the net charge of dissociated cellulose can play a significant role in the dissolution of this polymer (Kihlman et al. 2013).

Cellulose dissolution in aqueous NaOH and the stability of the solution against gelation can be enhanced with certain additives, such as zinc oxide (ZnO) (Kihlman et al. 2013; Liu et al. 2011; Yang et al. 2011). Despite the clear improvement of cellulose solubility with the addition of ZnO observed in

practice, the exact role of the added ZnO is currently under debate. ZnO forms zincate ( $\text{Zn}(\text{OH})_4^{2-}$ ) in the strongly alkaline NaOH solution, and Yang et al. (2011) have suggested that the zincate improves cellulose dissolution by forming even stronger hydrogen bonds with it while Kihlman et al. (2013) have proposed that the zincate associates to cellulose enhancing the dissolution by further charging up the molecules. On the other hand, it might be that a Zn-cellulose complex is formed in the alkaline environment (Väisänen et al. 2021). Furthermore, Liu et al. (2011) have proposed that ZnO acts as water “binder” stabilizing cellulose solutions.

However, even with the addition of ZnO, dissolution of wood fibers is poor without a pretreatment, or “activation”, prior to the dissolution process (Cuissinat and Navard 2006; Kihlman et al. 2012; Väisänen et al. 2021). The high DP of cellulose has been shown to be one of the most important factors hindering its dissolution in the alkaline system (Isogai and Atalla 1998; Yamashiki et al. 1990; Yang et al. 2011). However, it is not the only factor affecting the dissolution. It has also been shown that in the cell wall, the longer the time from the cellulose deposition is, the more difficult it is to dissolve the cellulose (Le Moigne et al. 2008). In addition, thick-walled compression wood cells and summerwood cells might be difficult to dissolve (Jardeby et al. 2004). Thus, the structural organization of the cell wall layers and/or the presence of non-cellulosic material in the cell wall have an effect on the dissolution (Le Moigne et al. 2008; Le Moigne and Navard 2010). Indeed, when plant fibers are placed in the aqueous NaOH solvent, heterogeneous swelling along the fiber length, a phenomenon called “ballooning”, is observed. This phenomenon was discovered already a long time ago (Nägeli 1864). Based on more recent studies, Cuissinat and Navard (2008) have proposed the mechanism for dissolution by ballooning to be the following: when the solvent permeates the fibers, cellulose in the secondary wall dissolves causing heterogeneous swelling of the primary wall and the formation of balloons finally bursting them followed by the dissolution of the unswollen sections of the fibers and, in the end, the balloon membrane scraps. In order to enhance the dissolution of cellulosic fibers many types of pretreatment methods have been employed including steam explosion, hydrothermal, chemical and enzymatic treatments (Kihlman et al. 2012, 2013; Le

Moigne and Navard 2010; Peleteiro et al. 2015; Trygg and Fardim 2011; Yamashiki et al. 1990; Wawro et al. 2009).

In this paper, the effect of various hydrolytic pretreatments on wood pulp dissolution in the aqueous NaOH–ZnO solvent system is investigated. The dissolution of the pulps is evaluated both visually with an optical microscope as well as at the molecular level based on their reactivity with 4-acetamido-2,2,6,6-tetramethylpiperidine-1-oxo-piperidium (4-AcNH-TEMPO<sup>+</sup>). The method for studying the reactivity of cellulose is based on rapid and selective oxidation of the hydroxymethyl (–CH<sub>2</sub>OH) groups of cellulose to carboxyl groups (–COOH) by 4-AcNH-TEMPO<sup>+</sup> in mild conditions (pH 9, room temperature) (Khanjani et al. 2017; Väisänen et al. 2021). The method enables studying the reactivity of cellulose quantitatively and thus assessing the dissolution at the molecular level. In theory, fully dissolved (molecularly dispersed) cellulose molecules should be able to react freely with 4-AcNH-TEMPO<sup>+</sup> resulting in complete oxidation of the –CH<sub>2</sub>OH groups of cellulose. Finally, pulp dissolution was evaluated in relation to the fiber properties (i.e. the extent of fibrillation, amount of fines and fiber width, coarseness, and length) as well as the hemicellulose and cellulose contents and the viscosity of the pulps.

## Materials and methods

### Materials

Eight pulps were obtained from UPM-Kymmene Corporation. They consisted of seven samples of a never-dried, bleached softwood (mixture of Scots pine and Norway spruce) kraft pulp that had undergone hydrolytic pretreatments under various conditions and the same pulp without a pretreatment as a reference. The samples were marked according to the consistency of the pulp in the hydrolysis and the final viscosity of the sample. Three samples, MC440, MC320 and MC220, were hydrolyzed at medium consistency (10%) in a batch reactor at 160 °C under continuous stirring. The pH of the sample MC220 was adjusted to 3 with acetic acid before heating. The rest of the hydrolyzed samples, HC350, HC336, HC250 and HC224, were hydrolyzed at high consistency (50%) in a continuous reactor where the pulp slurry

was fed with a plug screw. The reactor was heated to 170 °C with steam. The pH of the slurry was adjusted to 3.3 with sulfuric acid before feeding it to the reactor. It should be noted that the processing conditions of the pulp HC250 were exactly the same as those of the pulp HC224. The only difference between these samples is that HC250 was mechanically refined after the hydrolysis. The hydrolysis conditions are listed in more detail in Table 1. The viscosities of the pulps were studied in cupriethylenediamine (CED) according to the standard ISO 5351 and the fiber properties were analyzed by Valmet FS5 Fiber Image Analyzer. These values were measured at the mill and they are shown in Table 2.

The pulps were dissolved with NaOH (purity 99.6%) purchased from VWR Chemicals and ZnO (pro analysis) from Merck. For the acetone extraction, acetone (purity ≥ 99.8%) from VWR chemicals was used. The reactivity of the pulps was studied with 4-acetamido-2,2,6,6-tetramethylpiperidine-1-oxo-piperidium (4-AcNH-TEMPO<sup>+</sup>) tetrafluoroborate (purity 97%) and pH 2 buffer solution (AVS titrinorm) purchased from Sigma-Aldrich and VWR Chemicals, respectively. In addition, boric acid (purity > 99.8%) from Sigma Aldrich and NaOH (purity 99.6%) from VWR Chemicals were used to prepare the pH 9 buffer solution. All dilutions were done in Milli-Q water (Millipore Corporation, resistivity 18.2 MΩ cm).

### Determination of structural carbohydrates

To remove any extractives from the pulps, they were dried in an oven at 40 °C for overnight, ground and extracted with acetone for 6 h using a Soxhlet setup prior to their structural carbohydrate (cellulose and hemicelluloses) contents analysis. The structural carbohydrates contents of the pulps were determined according to the U.S. National Renewable Energy Laboratory (NREL) analytical procedure NREL/TP-510-42618 (Sluiter et al. 2008). The samples were hydrolyzed to their constituent monosaccharides with 72% sulfuric acid (H<sub>2</sub>SO<sub>4</sub>), filtered through a filtering crucible and analyzed using high-performance anion-exchange chromatography with pulsed amperometric detection (HPAEC-PAD) in a Dionex ICS-3000 system (Thermo Fisher Scientific) with a CarboPac PA20 column and MilliQ-water as the eluent. The cellulose and hemicellulose contents of the pulps were

**Table 1** The conditions of the hydrolytic pretreatments of the studied pulps

Pulp	Consistency	Temperature (°C)	Time (min)	pH	Viscosity (ml/g)
MC440	Medium	160	25	4 <sup>a</sup>	440
MC320	Medium	160	50	4 <sup>a</sup>	320
MC220	Medium	160	10	3	220
HC350	High	170	10	3.3	350
HC336	High	170	20	3.3	336
HC224	High	170	50	3.3	224
HC250 <sup>b</sup>	High	170	50	3.3	250

<sup>a</sup>Hydrothermal treatment, no acid added

<sup>b</sup>Same pretreatment as for HC224 but the fibers were mechanically refined after the process

**Table 2** The fiber properties, viscosities, cellulose and hemicellulose contents as well as the reactivities of the studied pulps

Pulp	Fiber properties					Reactivity (mmol/g)	Structural carbohydrates		
	Fibrillation (%)	Fines, 0–0.2 mm (%)	Width (μm)	Coarseness (mg/m)	Length (mm)		CEL (%)	XYL (%)	GLM (%)
MC440	1.15	4.5	20.5	0.19	1.91	4.16	83.9	8.2	7.9
MC320	1.21	6.0	20.6	0.19	1.74	4.39	84.8	7.8	7.4
MC220	1.29	6.0	20.1	0.18	1.69	5.14	84.9	7.5	7.6
HC350	1.30	6.4	19.8	0.18	1.71	4.33	84.7	7.1	8.2
HC336	1.30	6.6	19.8	0.17	1.70	4.24	85.5	7.1	7.3
HC224	1.27	7.3	19.0	0.16	1.33	3.76	82.8	9.5	7.7
HC250	N/A	N/A	N/A	N/A	N/A	4.59	85.3	7.7	7.0
REF	N/A	N/A	N/A	N/A	N/A	4.10	83.0	9.3	7.8

calculated from the monosaccharides according to the formula published by Janson (1970).

### Dissolution and imaging

4 wt% sample (dry matter) was dissolved in the solvent system containing 9 wt% NaOH and 1 wt% ZnO. NaOH and ZnO were first dissolved in the mass ratio of 6:1 (18 wt% in total) in boiling water in order to dissolve the ZnO and the solution was then cooled to – 10 °C in an ice-salt bath. The pulps were activated in Milli-Q water in a separate container and then mixed with the NaOH–ZnO solution. The mixture was stirred with a mechanical stirrer in the ice-salt bath for 10 min.

All of the samples were visually studied with a Leica ICC50 HD microscope. Images of the pulps were taken before and immediately after their dissolution in the NaOH–ZnO system as well as after storing the solutions in the fridge for 24 h to see whether the samples changed over time.

### Oxidation with 4-AcNH-TEMPO<sup>+</sup>

The reactivity of the pulps dissolved in the NaOH–ZnO solvent system was studied based on their oxidation with 4-AcNH-TEMPO<sup>+</sup> according to the method published before (Khanjani et al. 2017). The samples were oxidized at room temperature in pH 9 buffer solution under continuous mixing and the consumption of 4-AcNH-TEMPO<sup>+</sup> was monitored with absorption spectrophotometry based on its reaction with potassium iodide (KI) (Bichsel and von Gunten 1999; Pääkkönen et al. 2015).

The total volume of the reaction mixture was 100 ml and the amount of 4-AcNH-TEMPO<sup>+</sup> added was 2.5 mmol/l. The amount of pulp analyzed in each experiment was 0.05 g/l. These dosages were chosen according to a previous study (Väisänen et al. 2021). For monitoring the consumption of 4-AcNH-TEMPO<sup>+</sup>, 1 ml aliquots of the reaction mixture were taken, mixed with 1 ml of 10% KI solution and diluted to 40 ml with pH 2 buffer solution. The absorption

spectrum of the solution was recorded with a spectrophotometer (Shimadzu UV-2550) at appropriate time intervals. The recording of time was started immediately after mixing the samples with the 4-AcNH-TEMPO<sup>+</sup>. Finally, the values for reactivity (mmol/g) were obtained by nonlinear fitting of the oxidant decay data. The procedure is explained in more detail before (Khanjani et al. 2017; Väisänen et al. 2021).

## Results and discussion

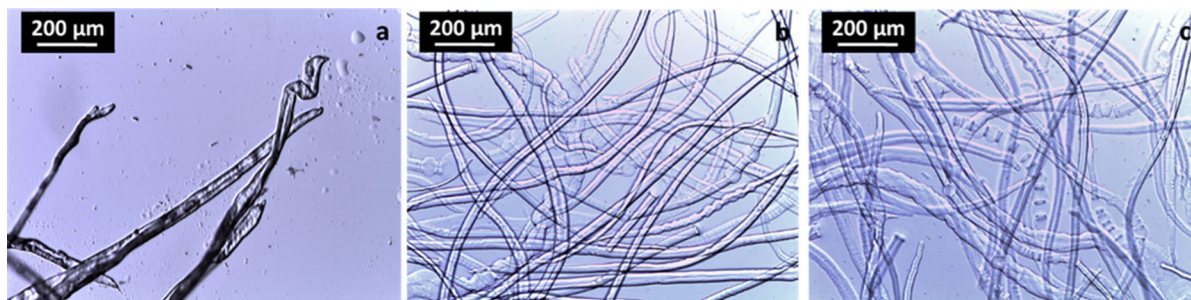
### Pulp dissolution and gelation in aqueous NaOH–ZnO

Figures 1, 2, 3 and 4 show the microscope images of the reference pulp, medium consistency hydrolyzed pulps, high consistency hydrolyzed pulps and the high consistency hydrolyzed pulp with mechanical refining, HC250, respectively. The figures contain images of the pulps before and immediately after their dissolution in the NaOH–ZnO system as well as 24 h after it to see whether the samples have changed within 24 h.

The unhydrolyzed reference pulp was formed of intact fibers with no fibrillation (Fig. 1a). Some fibers had kinks. The pulp formed an opaque gel in NaOH–ZnO. The fibers were mostly intact with some ballooning indicating that the solvent was able to penetrate the fibers only partly causing partial swelling and ballooning (Fig. 1b). Thus, the dissolution of the unhydrolyzed reference pulp was poor. After storing the sample in the fridge for 24 h, the fibers fell to the bottom of the flask leaving a layer of solvent on top of the gel. The appearance of the fibers under the

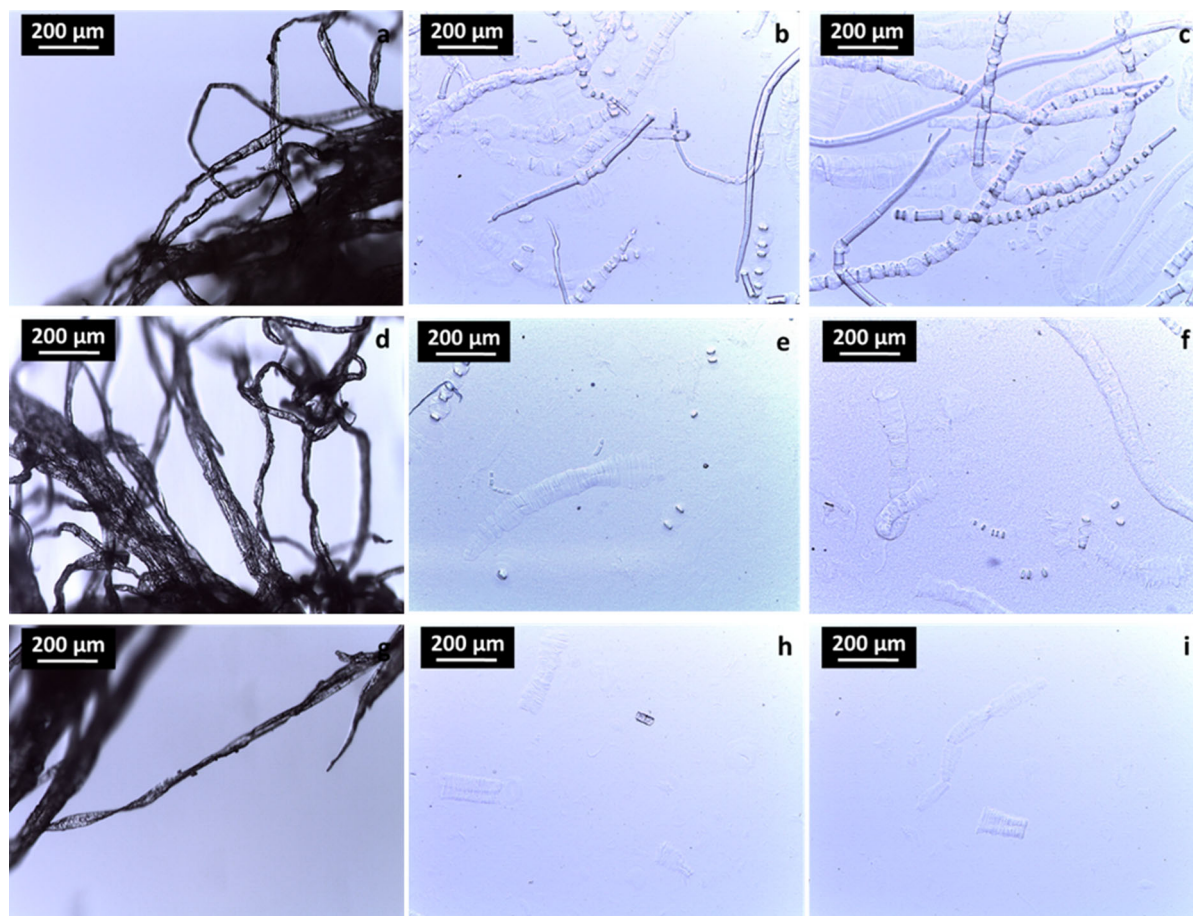
microscope remained unchanged (Fig. 1c). The poor dissolution of the untreated softwood pulp was expected. It is well known that aqueous NaOH is not a good solvent for wood pulp fibers that have undergone no pretreatment or “activation” (Le Moigne and Navard 2010). Moreover, it has been shown before that even with added ZnO, the system is not able to dissolve softwood pulp without any pretreatments (Kihlman et al. 2012; Väisänen et al. 2021).

Figure 2 shows microscope images of the medium consistency hydrolyzed pulps. The widths of these fibers appeared to be on the average smaller than the widths of the untreated reference fibers (Fig. 2a, d, g). Moreover, the fibers of MC440 and MC320 were intact with no fibrillation (Fig. 2a, d). Curls, kinks and some twists were observed. The fibers of MC220 looked similar to the other medium consistency hydrolyzed pulps except that MC220 consisted also of a small fraction of fibrillated fibers as well as loose fibrils and fiber fragments, and some of the intact fibers had fines on their surface (Fig. 2g). In NaOH–ZnO, MC440 formed a translucent gel. The sample contained some highly swollen fibers, some ballooned fibers and also single fibers that were still intact indicating that the solvent was able to penetrate the fibers and only partially dissolve them (Fig. 2b). No change was observed in the sample within storing it in the fridge for 24 h. During the dissolution process, MC320 formed a translucent, sticky gel that had an interesting glue-like consistency. Some ballooned and some highly swollen fiber sections as well as small highly swollen fiber fragments were observed with the microscope in addition to single parts of fibers that were still intact (Fig. 2e). Thus, the solvent was able to permeate the fibers of MC320 and dissolve them



**Fig. 1** Microscope images of the never-dried, bleached softwood reference pulp before its dissolution in aqueous NaOH–ZnO (a), immediately after it (b) and 24 h after it (c)





**Fig. 2** Microscope images of the medium consistency hydrolyzed pulps before their dissolution in aqueous NaOH–ZnO, immediately after it and 24 h after it: samples MC440 (a, b, c), MC320 (d, e, f) and MC220 (g, h, i), respectively

mostly leaving only fragments of fibers undissolved. No change was observed in the sample within 24 h. MC220 dissolved in the NaOH–ZnO solvent system formed a translucent, viscous liquid. A few highly swollen fiber sections as well as a lot of small fiber fragments together with a very few barely visible flat rings with outer diameters of 50–100  $\mu\text{m}$  and inner diameters of 20–50  $\mu\text{m}$  were observed under the microscope in addition to single small parts of fibers that were still intact (Fig. 2h). Thus, the solvent was able to permeate the fibers and dissolve them mostly leaving only small highly swollen fragments of fibers visible in the microscope images. The sample turned into a gel within 24 h.

Similar to the medium consistency hydrolyzed pulps, the fibers of the high consistency pulps looked narrower than the untreated fibers of the reference pulp and they also had kinks and curls (Fig. 3a, d, g).

However, these fibers showed more twisting around themselves as well as around other fibers compared to the medium consistency hydrolyzed pulps. The fibers looked mostly intact with a little amount of fibrillation observed in some of the fibers in each of the high consistency hydrolyzed pulps. In NaOH–ZnO, HC350 formed a translucent liquid that turned into a gel when the temperature of the sample was increased to room temperature. The microscope images showed highly swollen fibers, fiber sections and small fiber fragments as well as few flat rings with outer diameter of ca. 100  $\mu\text{m}$  and inner diameter of 20–50  $\mu\text{m}$  (Fig. 3b) indicating that the solvent was able to swell the fibers and dissolve them partially. The gel turned more viscous within 24 h. The appearance of HC336 in NaOH–ZnO was similar to the appearance of the HC350 in NaOH–ZnO being a translucent liquid, however, it did not gel when warmed up to room

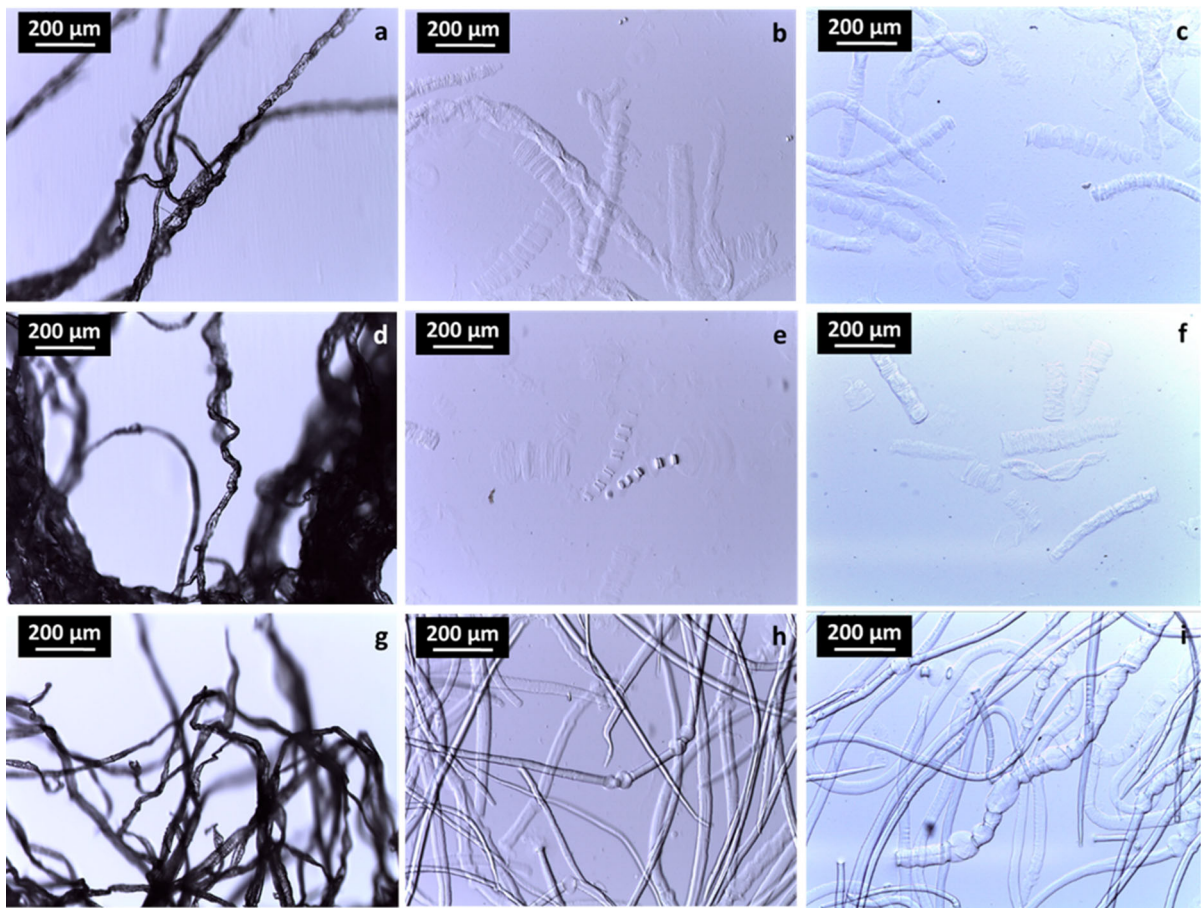


**Fig. 3** Microscope images of the high consistency hydrolyzed pulps before their dissolution in aqueous NaOH–ZnO, immediately after it and 24 h after it: samples HC350 (a, b, c), HC336 (d, e, f) and HC224 (g, h, i), respectively

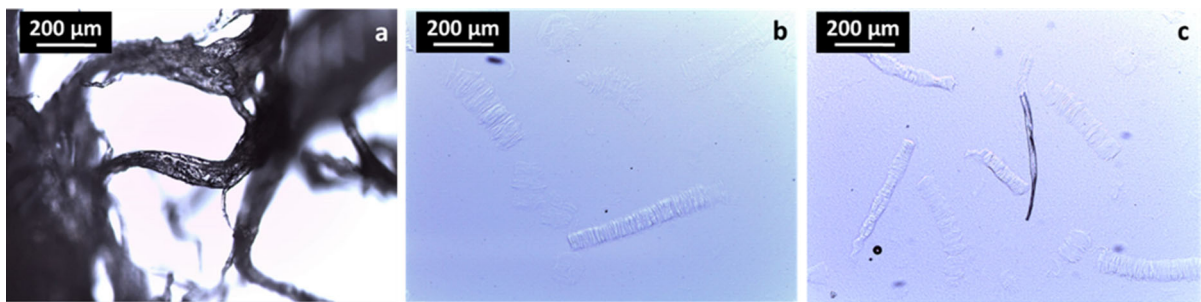


**Fig. 4** Microscope images of the high consistency hydrolyzed pulp whose fibers have been mechanically refined after the hydrolysis, HC250, before its dissolution in aqueous NaOH–ZnO (a), immediately after it (b) and 24 h after it (c)

temperature. The microscope images of HC336 in NaOH–ZnO showed smaller sections of highly swollen fibers compared to the HC350 in NaOH–ZnO and a few flat rings with outer diameter of 50–100  $\mu\text{m}$  and inner diameter of 20–50  $\mu\text{m}$ . However, it contained

some ballooned, partially dissolved fiber sections that were not observed for HC350 (Fig. 3e). Thus, the solvent was able to permeate the fibers and dissolve them mostly. However, the action of the solvent was uneven as some partially dissolved, ballooned fiber



parts were observed. The sample did not change within 24 h. HC224 was different from HC350 and HC336 as it formed an opaque gel during the dissolution process. HC224 in NaOH–ZnO contained a lot of fibers that still looked intact (Fig. 3h). In addition, some fibers with a little ballooning, a few highly swollen fibers and no small fiber fragments were visible. It is clear that the solvent was able to permeate the fibers only partially causing partial swelling but leaving many fibers intact. No change was observed within 24 h. The fibers formed aggregates during the hydrolysis of the sample HC224 and thus it was decided to further refine it mechanically forming another sample, HC250. In the microscope images, the fibers of HC250 looked partly damaged and had pieces ripped of the cell wall (Fig. 4a). In NaOH–ZnO, the pulp formed a translucent sticky gel with a glue-like consistency. Microscope images revealed that the solvent was able to dissolve the fibers mostly. Only some swollen fiber sections and a few barely visible small fiber fragments were observed in the microscope images (Fig. 4b). The sample did not change within 24 h.

As discussed above, there were clear differences in the dissolution behavior of the pulps with different hydrolytic pretreatments. However, all of the pulps showed uneven action of the solvent and some undissolved matter was visible even in the microscope images of the best dissolved pulps. The phenomenon of uneven dissolution of cellulose fibers in aqueous NaOH is well known and it has been linked to the structure of the fiber wall and the chemical environment of cellulose chains in it (Le Moigne and Navard 2010). The ballooning phenomenon observed for the pulps MC440, MC320, HC336, HC224, and the reference pulp has been linked to the swelling and dissolution of the secondary wall inducing the breaking of the primary wall, which in turn results in the formation of unswollen sections and thick helices (Le Moigne et al. 2008). Thus, the observation of ballooned fibers indicates that the external cell wall layers are still present in these fibers (Le Moigne and Navard 2010). On the other hand, highly and homogeneously swollen fibers and fiber parts were observed for all of the pulps in NaOH–ZnO except for the pulp HC224 and the reference pulp. Le Moigne and Navard (2010) have suggested that the high swelling along the fibers without unswollen sections and helices is induced by the secondary cell wall and that it indicates that the primary cell wall is not present anymore. The

flat rings similar to what was observed for the pulps MC220, HC350 and HC336 in NaOH–ZnO have been suggested to originate from ballooned fibers or swelled pores (Jardeby et al. 2005) or, alternatively, cutting of the highly swollen fibers (Le Moigne and Navard 2010).

#### Effect of pretreatment on dissolution

The reactivities of the dissolved fibers can be used to evaluate their dissolution quantitatively at the molecular level. In theory, fully dissolved, molecularly dispersed cellulose molecules should be fully available to react with 4-AcNH-TEMPO<sup>+</sup> and thus have all the hydroxymethyl groups oxidized in the excess of 4-AcNH-TEMPO<sup>+</sup>. When comparing the reactivities of the medium consistency autohydrolyzed pulps MC440 and MC320 (Table 2), it is observed that increasing the hydrolysis time from 25 to 50 min resulted in better dissolution shown as higher reactivity. However, when the pH was adjusted to 3, only 10 min was enough to achieve even better dissolution as observed for MC220. On the contrary, the dissolution of the high consistency hydrolyzed pulps became poorer with increasing hydrolysis time as observed from the decreasing reactivities of the pulps HC350, HC336 and HC224. In fact, with the hydrolysis time of 50 min (HC224), the reactivity of the pulp was lower than the reference. As already mentioned, formation of fiber aggregates was observed during the high consistency hydrolysis. The low pH, high temperature, long treatment time and possibly also the high consistency of the hydrolytic pretreatment may have induced fiber hornification. After mechanical refining, the dissolution power of the solvent increased significantly which is shown as the highest reactivity value for HC250 of all the high consistency hydrolyzed pulps.

In addition to the reactivities, fiber properties, viscosities and the structural carbohydrate contents (cellulose and hemicelluloses) of the pulps were determined. Increased hydrolysis time resulted in an increase in the amount of fibrillation and fines in the case of the medium consistency autohydrolyzed pulps MC440 and MC320 which were continuously mixed with a mechanical stirrer during the hydrolysis while a significantly smaller increase in these parameters was observed with time for the high consistency hydrolyzed pulps which were lacking mechanical mixing

during the hydrolysis (Table 2). Moreover, hornification leads to a decrease in the width and length of the fibers. The lowest fiber width and length are observed for HC224 indicating that the extent of hornification of this pulp is the highest of the studied pulps. Fiber coarseness, on the other hand, can be linked to yield loss. A decrease in pH for the medium consistency hydrolysis and an increase in time for the high consistency hydrolysis result in a slight decrease in the fibers' coarseness and, thus, slightly increased yield losses (Table 2). There is no doubt that the fiber properties, especially the intactness of the cell wall, affect the dissolution of the fibers, yet no correlation was found between any single fiber property and the solubility of the studied pulps. Thus, no single fiber property solely can be used to explain the dissolution power of the solvent on the pulps. The same conclusion has been reported before on fiber dissolution in aqueous NaOH solvents (Kihlman et al. 2012).

According to thermodynamics, the solubility of polymers normally increases with decreasing DP (viscosity) as the entropic term becomes larger with increased number of molecules in the solution. Indeed, cellulose DP has been reported to be an important factor explaining its dissolution (Isogai and Atalla 1998; Yamashiki et al. 1990; Yang et al. 2011). The viscosities of the studied pulps are shown in Fig. 5 as a function of the degree of oxidation of hydroxymethyl groups calculated from their fast reaction with 4-AcNH-TEMPO<sup>+</sup>. The hemicellulose content of the

pulps is taken into consideration in the calculation of the degrees of oxidation. As can be seen from Fig. 5, the dissolution power of the solvent increased with decreasing viscosities except for the most hornified and aggregated high consistency hydrolyzed pulp HC224 whose solubility decreased over time despite the reduction in viscosity. It should be noted here that due to the resistant nature of this pulp, it is possible that it did not dissolve completely during the carbohydrate content analysis either leaving some cellulose undetected which is shown by the unusually low cellulose content observed for HC224 in Table 2. Mechanical refining, however, restored its solubility to a level expected based on its viscosity as is seen for HC250 in Fig. 5. Moreover, as observed from Fig. 5 the degree of oxidation of the unhydrolyzed reference pulp was high (> 70%) despite its poor dissolution in the NaOH–ZnO system. The solvent has been able to disrupt the crystalline structure of cellulose in the S<sub>2</sub> layer leaving the outer layers of the fiber wall intact. Dissolution of the more resistant outer layers of the fiber wall are needed in order to fully dissolve the fiber (Le Moigne and Navard 2010). It has been shown before that the S<sub>1</sub> layer consists of helical bundles of elementary fibrils (Reza et al. 2017). Due to this “rope-like” arrangement of fibrils, detaching individual cellulose chains from each other is physically very difficult and a reduction in the DP of cellulose is needed in order to dissolve it. According to Fig. 5, the fibers start to dissolve when the viscosity is below ca. 400 ml/g (i.e. DP = ~ 550). After this value, a decrease in the viscosity of the pulp leads to an increase in the degree of oxidation (i.e. better dissolution) of the fibers. On the contrary, in the case of the high viscosity values, even a large decrease in viscosity has only a minor effect on the degree of oxidation. As is observed from Fig. 5, a reduction in viscosity from 750 ml/g measured for the unhydrolyzed pulp to 440 ml/g leads to a minor increase in the degree of oxidation despite the hydrolytic treatment that was done for the fibers. These results are in good agreement with the structure proposed by Reza et al. (2017). If the length of one cellobiose unit is 1.038 nm (Nishiyama et al. 2002), the length of a cellulose molecule with the DP of 550 is ca. 280 nm, which is below the mean period of the helical twists in the elementary fibril bundles in the S<sub>1</sub> layer, i.e.  $321 \pm 8$  nm, approximated by Reza et al. (2017).

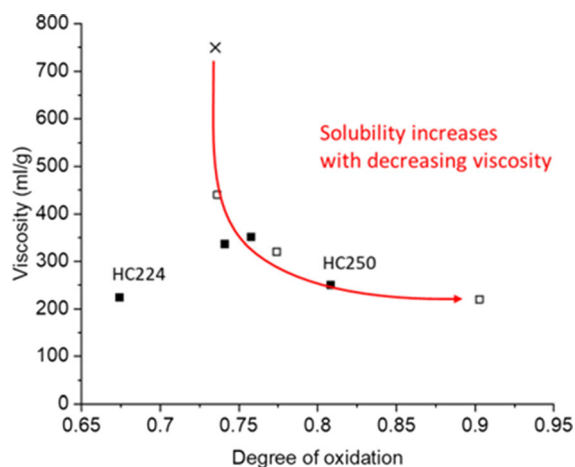


**Fig. 5** Viscosities of the pulps as a function of the degree of oxidation. The white and black squares and the cross represent the medium and high consistency hydrolyzed pulps as well as the unhydrolyzed reference pulp, respectively

Besides the DP, the hemicellulose content of the pulp, has been reported to negatively correlate with its solubility (Kihlman et al. 2012). Especially the mannans seem to hinder the solubility of cellulose which is explained by their high affinity to cellulose creating aggregates with it (Iwata et al. 1998; Le Moigne and Navard 2010; Salmén and Olsson 1998). In our study, the correlation between the total hemicellulose or glucomannan contents and the solubility of the pulps could not be confirmed when comparing all the pulps with the various hydrolytic treatments against each other. However, the glucomannan content of the pulps might have affected their tendency for gelation. This phenomenon can be observed when comparing the pulps HC350 and HC336 with viscosities close to each other. HC350 containing a higher amount of glucomannan formed a gel when warmed up to room temperature while HC336 did not. Another similar case can be found among the pulps with the highest solubilities, MC220 and HC250. Both of them dissolved well in the NaOH–ZnO system confirmed by optical microscopy as well as their reactivities with 4-AcNH-TEMPO<sup>+</sup>. However, after 24 h storage in the fridge, MC220 with the higher glucomannan content had formed a gel while HC250, despite its higher viscosity, had not.

## Conclusions

The effect of various types of hydrolytic pretreatments on alkaline dissolution of a never-dried softwood kraft pulp was studied. The dissolution of the pulps in the NaOH–ZnO solvent system was evaluated both visually with optical microscopy and at the molecular level based on their reactivity with 4-AcNH-TEMPO<sup>+</sup>. The medium consistency hydrolysis was successful in increasing the solubility of the fibers. The high consistency hydrolysis increased fiber solubility to some extent but with extended treatment time (50 min) the fibers formed aggregates and their dissolution became poor. This phenomenon could be overcome by mechanical refining of the fibers after the hydrolysis. Moreover, the unhydrolyzed reference pulp had a high degree of oxidation when reacting with 4-AcNH-TEMPO<sup>+</sup> (> 70%) despite its poor dissolution in the NaOH–ZnO system. Thus, it seems that the solvent is able to disrupt cellulose crystallinity in the S<sub>2</sub> layer causing this pulp to swell but not

dissolve. For complete dissolution of the fibers, dissolution of the more resistant outer layers of the fiber wall are needed. Comparison of the pulp viscosities over their degree of oxidation showed that the pulp started to dissolve when the viscosity was decreased to below ca. 400 ml/g (i.e. DP = ~ 550). This is in line with the fiber wall structure in the S<sub>1</sub> layer consisting of elementary fibrils assembled in helical bundles. The length of cellulose chains with the DP of 550 is below the mean period of the helical twists in the bundles. Thus, it seems that in order to detach individual cellulose chains from each other, they need to be short enough to overcome the physical barrier formed by the helical twists of the fibril bundles in the S<sub>1</sub> layer. The highest solubilities of the studied pulps were observed for the medium consistency hydrolyzed pulp MC220 reaching over 90% degree of oxidation and the high consistency hydrolyzed pulp after the mechanical refining, HC250, with the degree of oxidation over 80%. Furthermore, when pulps with similar viscosities were compared against each other, the ones with the higher glucomannan contents formed gels over time. This was observed also for the pulp MC220 with the lowest viscosity and the highest solubility of the studied pulps.

**Acknowledgments** This work was done in collaboration between UPM-Kymmene Corporation and Aalto University. The research team is thanked for the fruitful discussions at the project meetings. In addition, we are grateful for the support from Business Finland, Walter Ahlström foundation and the FinnCERES Materials Bioeconomy Ecosystem. Finally, M.Sc. Rubina Ajdary is highly thanked for her work in optimizing the dissolution system and Mrs. Rita Hatakka for her assistance with the HPAEC measurements.

**Funding** Open access funding provided by Aalto University. This work was a part of a joint research project between UPM-Kymmene Oyj and Aalto University. In addition, the authors would like to acknowledge the financial support from Business Finland, Walter Ahlström foundation and the FinnCERES Materials Bioeconomy Ecosystem.

**Data availability** The data that support the findings of this study are available from the corresponding author upon reasonable request.

**Code availability** Not applicable.

**Declarations**

**Conflict of interest** The authors declare no conflict of interest.

**Open Access** This article is licensed under a Creative Commons Attribution 4.0 International License, which permits use, sharing, adaptation, distribution and reproduction in any medium or format, as long as you give appropriate credit to the original author(s) and the source, provide a link to the Creative Commons licence, and indicate if changes were made. The images or other third party material in this article are included in the article's Creative Commons licence, unless indicated otherwise in a credit line to the material. If material is not included in the article's Creative Commons licence and your intended use is not permitted by statutory regulation or exceeds the permitted use, you will need to obtain permission directly from the copyright holder. To view a copy of this licence, visit <http://creativecommons.org/licenses/by/4.0/>.

## References

- Bialik E, Stenqvist B, Feng Y, Östlund Å, Furó I, Lindman B, Lund M, Bernin D (2016) Ionization of cellobiose in aqueous alkali and the mechanism of cellulose dissolution. *J Phys Chem Lett* 7:5044–5048. <https://doi.org/10.1021/acs.jpclett.6b02346>
- Bichsel Y, von Gunten U (1999) Determination of iodide and iodate by ion chromatography with postcolumn reaction and UV/visible detection. *Anal Chem* 71:34–38. <https://doi.org/10.1021/ac980658j>
- Budtova T, Navard P (2016) Cellulose in NaOH–water based solvents: a review. *Cellulose* 23:5–55. <https://doi.org/10.1007/s10570-015-0779-8>
- Cai J, Zhang L, Liu S, Liu Y, Xu X, Chen X, Chu B, Guo X, Xu J, Cheng H, Han CC, Kuga S (2008) Dynamic self-assembly induced rapid dissolution of cellulose at low temperatures. *Macromolecules* 41:9345–9351. <https://doi.org/10.1021/ma801110g>
- Cuissinat C, Navard P (2006) Swelling and dissolution of cellulose part II: free floating cotton and wood fibres in NaOH–water-additives systems. *Macromol Symp* 244:19–30. <https://doi.org/10.1002/masy.200651202>
- Cuissinat C, Navard P (2008) Swelling and dissolution of cellulose, part III: plant fibres in aqueous systems. *Cellulose* 15:67–74. <https://doi.org/10.1007/s10570-007-9158-4>
- Davidson GF (1934) The dissolution of chemically modified cotton cellulose in alkaline solutions. Part I: in solutions of sodium hydroxide, particularly at temperatures below the normal. *J Text Inst* 25:T174–T196. <https://doi.org/10.1080/19447023408661621>
- Davidson GF (1936) The dissolution of chemically modified cotton cellulose in alkaline solutions. Part II: a comparison of the solvent action of solutions of lithium, sodium, potassium and tetramethylammonium hydroxides. *J Text Inst* 27:T112–T130. <https://doi.org/10.1080/19447023608661674>
- Egal M, Budtova T, Navard P (2007) Structure of aqueous solutions of microcrystalline cellulose/sodium hydroxide below 0 °C and the limit of cellulose dissolution. *Biomacromol* 8:2282–2287. <https://doi.org/10.1021/bm0702399>
- Ghasemi M, Alexandridis P, Tsianou M (2017a) Cellulose dissolution: insights on the contributions of solvent-induced decrystallization and chain disentanglement. *Cellulose* 24:571–590. <https://doi.org/10.1007/s10570-016-1145-1>
- Ghasemi M, Tsianou M, Alexandridis P (2017b) Assessment of solvents for cellulose dissolution. *Bioresource Technol* 228:330–338. <https://doi.org/10.1016/j.biortech.2016.12.049>
- Hagman J, Gentile L, Jessen CM, Behrens M, Bergqvist K-E, Olsson U (2017) On the dissolution state of cellulose in cold alkali solutions. *Cellulose* 24:2003–2015. <https://doi.org/10.1007/s10570-017-1272-3>
- Huh E, Yang J-H, Lee C-H, Ahn I-S, Mhin BJ (2020) Thermodynamic analysis of cellulose complex in NaOH–urea using reference iteration site model. *Cellulose* 27:6767–6775. <https://doi.org/10.1007/s10570-020-03202-w>
- Isogai A (1997) NMR analysis of cellulose dissolved in aqueous NaOH solutions. *Cellulose* 4:99–107
- Isogai A, Atalla RH (1998) Dissolution of cellulose in aqueous NaOH solutions. *Cellulose* 5:309–319. <https://doi.org/10.1023/A:1009272632367>
- Iwata T, Indrarti L, Azuma J-I (1998) Affinity of hemicellulose for cellulose produced by *Acetobacter xylinum*. *Cellulose* 5:215–228. <https://doi.org/10.1023/A:1009237401548>
- Janson J (1970) Calculation of the polysaccharide composition of wood and pulp. *Paperi ja Puu* 52:323–329
- Jardebey K, Lennholm H, Germgård U (2004) Characterization of the undissolved residuals in CMC-solutions. *Cellulose* 11:195–202. <https://doi.org/10.1023/B:CELL.0000025390.81603.40>
- Jardebey K, Germgård U, Kreutz B, Heinze T, Heinze U, Lennholm H (2005) The influence of fibre wall thickness on the undissolved residuals in CMC solutions. *Cellulose* 12:167–175. <https://doi.org/10.1007/s10570-004-1371-9>
- Khanjani P, Väisänen S, Lovikka V, Nieminen K, Maloney T (2017) Assessing the reactivity of cellulose by oxidation with 4-acetamido-2,2,6,6-tetramethylpiperidine-1-oxo-piperidium cation under mild conditions. *Carbohydr polym* 176:293–298. <https://doi.org/10.1016/j.carbpol.2017.08.092>
- Kihlman M, Aldaeus F, Chedid F, Germgård U (2012) Effect of various pulp properties on the solubility of cellulose in sodium hydroxide solutions. *Holzforschung* 66:601–606. <https://doi.org/10.1515/hf-2011-0220>
- Kihlman M, Medronho BF, Romano AL, Germgård U, Lindman B (2013) Cellulose dissolution in an alkali based solvent: influence of additives and pretreatments. *J Baz Chem Soc* 24:295–303. <https://doi.org/10.5935/0103-5053.20130038>
- Le Moigne N, Navard P (2010) Dissolution mechanisms of wood cellulose fibers in NaOH–water. *Cellulose* 17:31–45. <https://doi.org/10.1007/s10570-009-9370-5>
- Le Moigne N, Montes E, Pannetier C, Höfte H, Navard P (2008) Gradient in dissolution capacity of successively deposited cell wall layers in cotton fibres. *Macromol Symp* 262:65–71. <https://doi.org/10.1002/masy.200850207>
- Lindman B, Karlström G, Stigsson L (2010) On the mechanism of dissolution of cellulose. *J Mol Liq* 156:76–81. <https://doi.org/10.1016/j.molliq.2010.04.016>
- Liu W, Budtova T, Navard P (2011) Influence of ZnO on the properties of dilute and semi-dilute cellulose–NaOH–water



- solutions. *Cellulose* 18:911–920. <https://doi.org/10.1007/s10570-011-9552-9>
- Medronho B, Lindman B (2015) Brief overview on cellulose dissolution and regeneration interactions and mechanisms. *Adv Colloid Interfac* 222:502–508. <https://doi.org/10.1016/j.cis.2014.05.004>
- Nägeli C (1864) Ueber den inneren Bau der vegetabilischen Zellenmembranen Sitzber. Bay Akad Wiss Munchen 1:282–323
- Nishiyama Y, Langan P, Chanzy H (2002) Crystal structure and hydrogen-bonding system in cellulose I $\beta$  from synchrotron X-ray and neutron fiber diffraction. *J Am Chem Soc* 124:9074–9082. <https://doi.org/10.1021/ja0257319>
- Pääkkönen T, Bertinetto C, Pönni R, Tummala GK, Nuopponen M, Vuorinen T (2015) Rate-limiting steps in bromide-free TEMPO-mediated oxidation of cellulose—quantification of the N-oxoammonium cation by iodometric titration and UV-vis spectroscopy. *Appl Catal A* 505:532–538. <https://doi.org/10.1016/j.apcata.2015.07.024>
- Peleteiro S, Rivas S, Alonso JL, Santos V, Parajó JC (2015) Utilization of ionic liquids in lignocellulose biorefineries as agents for separation, derivatization, fractionation, or pretreatment. *J Agric Food Chem* 63:8093–8102. <https://doi.org/10.1021/acs.jafc.5b03461>
- Pereira A, Duarte H, Nosrati P, Gubitosi M, Gentile L, Romano A, Medronho B, Olsson U (2018) Cellulose gelation in NaOH solutions is due to cellulose crystallization. *Cellulose* 25:3205–3210. <https://doi.org/10.1007/s10570-018-1794-3>
- Reza M, Bertinetto C, Ruokolainen J, Vuorinen T (2017) Cellulose elementary fibrils assemble into helical bundles in S1 layer of spruce tracheid wall. *Biomacromolecules* 18:374–378. <https://doi.org/10.1021/acs.biomac.6b01396>
- Roy C, Budtova T, Navard P (2003) Rheological properties and gelation of aqueous cellulose-NaOH solutions. *Biomacromolecules* 4:259–264. <https://doi.org/10.1021/bm020100s>
- Salmén L, Olsson A-M (1998) Interaction between hemicelluloses, lignin and cellulose: structure–property relationships. *J Pulp Pap Sci* 24:99–103
- Sluiter A, Hames B, Ruiz R, Scarlata C, Sluiter J, Templeton D, Crocker D (2008) Determination of structural carbohydrates and lignin in biomass. In: DOE (ed) National renewable energy laboratory. Technical report: NREL/TP-510-42618
- Trygg J, Fardim P (2011) Enhancement of cellulose dissolution in water-based solvent via ethanol-hydrochloric acid treatment. *Cellulose* 18:987–994. <https://doi.org/10.1007/s10570-011-9550-y>
- Väisänen S, Ajdary R, Altgen M, Nieminen K, Kesari KK, Ruokolainen J, Rojas OJ, Vuorinen T (2021) Cellulose dissolution in aqueous NaOH–ZnO: Cellulose reactivity and the role of ZnO. *Cellulose*. <https://doi.org/10.1007/s10570-020-03621-9>
- Wawro D, Steplewski W, Bodek A (2009) Manufacture of cellulose fibres from alkaline solutions of hydrothermally-treated cellulose pulp. *Fibres Text East Eur* 17:18–22
- Yamashiki T, Matsui T, Saitoh M, Okajima K, Kamide K, Sawada T (1990) Characterization of cellulose treated by the steam explosion method. Part 2: effect of treatment conditions on changes in morphology, degree of polymerization, solubility in aqueous sodium hydroxide, and supermolecular structure of soft wood pulp during steam explosion. *Br Polym J* 22:121–128. <https://doi.org/10.1002/pi.4980220111>
- Yang Q, Qi H, Lue A, Hu K, Cheng G, Zhang L (2011) Role of sodium zincate on cellulose dissolution in NaOH/urea aqueous solution at low temperature. *Carbohydr Polym* 83:1185–1191. <https://doi.org/10.1016/j.carbpol.2010.09.020>

**Publisher's Note** Springer Nature remains neutral with regard to jurisdictional claims in published maps and institutional affiliations.